JOURNAL OF GEOPHYSICAL RESEARCH, VOL. 106, NO. B2, PAGES 2221-2234, FEBRUARY 10, 2001

High-resolution geological record of historic earthquakes in the Dead Sea basin

Revital Ken-Tor, Amotz Agnon, Yehouda Enzel, and Mordechai Stein
Institute of Earth Sciences, The Hebrew University, Jerusalem

Shmuel Marco[1]
Geological Survey of Israel, Jerusalem, and Department of Geophysics, Tel Aviv University, Tel Aviv

Jorg F. W. Negendank
GeoForschungsZentrum Potsdam, Potsdam

Abstract A 2000 year paleoseismic record of the Dead Sea area was recovered from a lacustrine sedimentary section. The section is being exposed at the Ze'elim Terrace on the shores of the Dead Sea due to the fast retreat of the lake. The section consists of laminated detrital and chemical (mainly aragonite) sediments that were deposited in the Holocene paleo-Dead Sea. Eight layers in the section show deformed sedimentary structures and are identified as seismites. Their chronology was determined by radiocarbon dating on organic remains. The seismite ages are well correlated with the historically documented earthquakes of 64 and 31 B.C. and 33, 363, 1212, 1293, 1834 and 1927 A.D.. The few historically documented earthquakes that have no correlatives in the Ze'elim seismite record occurred in times of sedimentary hiatuses at this site (e.g., 749 A.D.). Based on modern analogues and the association of similar disturbed layers with syndepositional faults, the Ze'elim Terrace seismites indicate M>5.5 earthquakes. The average recurrence interval is estimated as ~100-300 years and represents slip events on different faults in the Dead Sea area. The Ze'elim section provides a unique opportunity to correlate two independent and extensive data sets, the historical and sedimentary records. This study opens the way for better understanding of spatial and temporal distribution of earthquakes along the Dead Sea Transform and elsewhere.

1. Introduction

Paleoseismic records provide essential data for seismic hazard assessment, imposing important constraints on the temporal and spatial distribution of strong and harmful earthquakes. Information on pre-instrumental paleoseismic events is derived from historical and geological records. The historical information is mainly based on eyewitness reports and their preservation, the objectivity of the reporters, and the accessibility of the reports to historians. The quality of the geological information depends on the availability of suitable sedimentary sequences and the possibility of obtaining absolute ages on the paleoseismic events.

The Dead Sea is located along one of the major strike-slip fault systems in the world, the Dead Sea Transform (DST), which has been active since the Neogene [*Garfunkel*, 1981; *Garfunkel and Ben-Avraham*, 1996] (Figure 1). The DST is part of the 6000 km long Syrian-African rift system, which was a main route of travel for prehistorical mankind on its migration out of Africa. and since then, the locus of various historical communities. Thus, the DST and its surroundings contain numerous archeological remains that record human settlement since early prehistoric time, throughout the Bronze and Iron ages and the historical period. Some of the archeological sites were disturbed by earthquakes and, together with historical accounts of felt earthquakes, they provide a unique opportunity to monitor past seismic activity in the region [*Ben-Menahem*, 1991].

During the Pleistocene and Holocene, laminated evaporitic and detrital sediments were deposited at the bottom of a series of lakes that existed along the DST. The deposits contain suitable material for dating by U-series and radiocarbon [*Schramm et al.*, 2000]. The well-exposed sedimentary record in the region represents a potentially rich source of paleoseismic information that has not been fully exploited. An excellent example of this potential is given by the Lisan Formation, which consists of ~ 50 kyr laminated sedimentary sequence that contains deformed units representing individual, datable seismic events [*Marco and Agnon*, 1995; *Marco et al.*, 1996]. The present study focuses on the paleoseismic record of the last 2000 years in the Dead Sea basin. During this time the level of the Dead Sea has been low (at ~ 400 m below sea level) and subjected to small lake level fluctuations. Continuous retreat of the Dead Sea during the past 40 years (~ 80 cm yr^{-1}) has exposed the Holocene sediments, allowing the study of their structure and composition. In this study, the late Holo-

[1] Also at Geological Survey of Israel, Jerusalem, Israel.

Paper number 2000JB900313.
0148-0227/01/2000JB900313$09.00

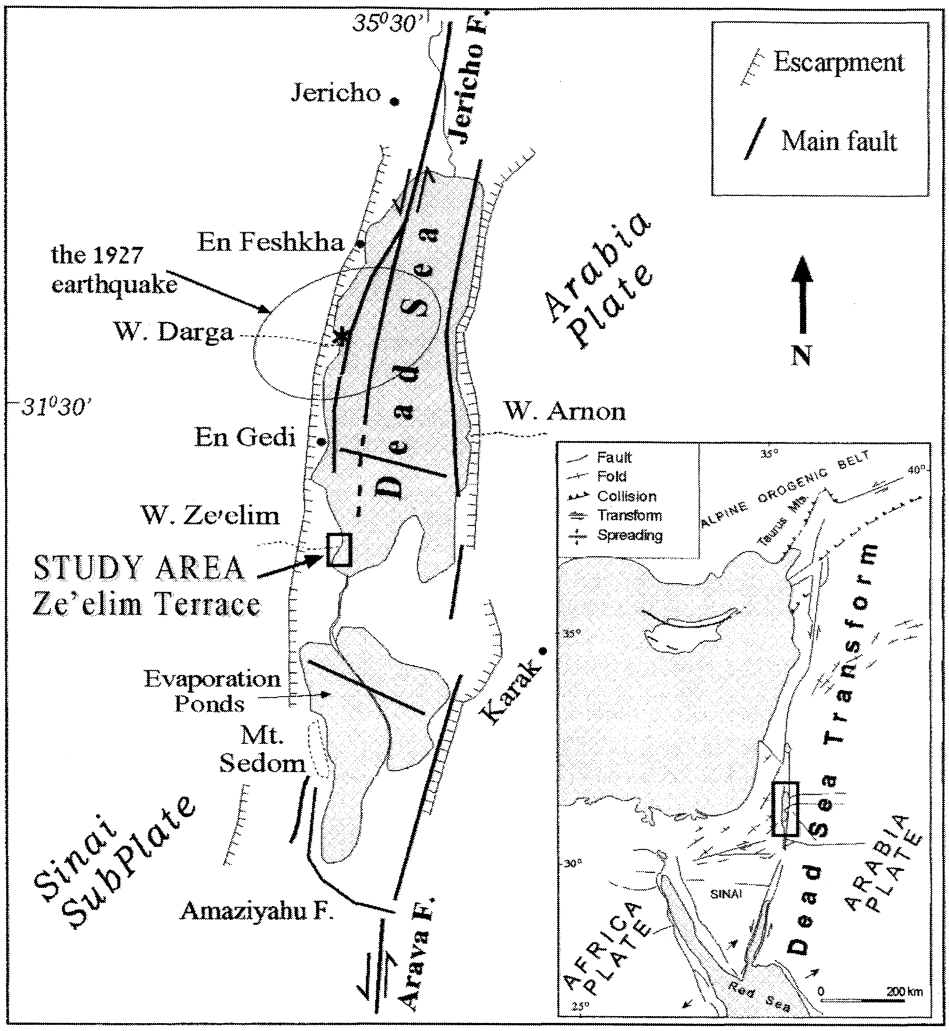

Figure 1. Location Map showing major faults in the Dead Sea region [*Garfunkel and Ben-Avraham*, 1996; *Garfunkel et al.*, 1981]. Also marked are the epicenter of the Jericho 1927 earthquake and its uncertainty ellipse [*Shapira et al.*, 1993]. Inset shows the general plate tectonic setting of the Dead Sea Transform.

cene sedimentary section exposed at the Ze'elim Terrace (Figure 1) is described. Several of the layers in this sequence contain features that are interpreted as seismically induced structures (seismites). The aim of this work is to document this paleoseismic record and to test its chronology against the historical earthquake record of the Dead Sea area.

2. The Ze'elim Formation

After the retreat of Lake Lisan at 17-13 kyr, the lake stabilized (for most of the time) at elevation of ~ 400 mbsl. [*Frumkin et al.*, 1991; *Neev and Emery*, 1995; *Kadan*, 1997]. Sediments deposited in this post-Lisan water body (or paleo-Dead Sea) compose the Ze'elim Formation [*Ken-Tor et al.*, 1998; *Migowski et al.*, 1999, *Yechieli*, 1993]. The Ze'elim Formation records the sedimentological, limnological, and tectonic history of the lake during the Holocene. It is exposed along the periphery of the Dead Sea and was recovered in several boreholes along the western shore of the lake [*Migowski et al.*, 1999]. The Ze'elim Formation consists of different lacustrine to fluvial sediments that reflect the lake-level fluctuations in the semiarid environment of the Dead Sea area. The thickness of the Holocene deposits reaches about 20-30 m at the western shore of the lake's northern basin [*Kadan*, 1997; *Migowski et al.*, 1999; *Yechieli et al.*, 1993], and about 80 m in the southern basin [*Neev and Emery*, 1995].

The Ze'elim Terrace (Figure 1) is incised by several gullies, up to a few meters deep and up to a few tens of meters wide (Plate 1a). Fieldwork was conducted in two gullies where approximately 7 m of the upper Ze'elim Formation are exposed. Figure 2 provides a composite section of the outcrops exposed in the two gullies. The depositional environment exposed in the northern gully is mainly lacustrine, while in the southern gully the depositional environments are shore and nearshore.

The section was divided into several lithological units. The lacustrine sediments consist of alternating aragonite and detrital laminae (~1-2 mm thick) and thicker clastic layers (>10cm). The aragonite precipitated chemically from the water column as was described for the Lisan Formation (cf. *Begin et al.*, 1974; *Stein et al.*, 1997). The detrital layers consist of clay- and silt-size grains of Cretaceous rocks exposed in the catchment area and therefore represent flood input that entered

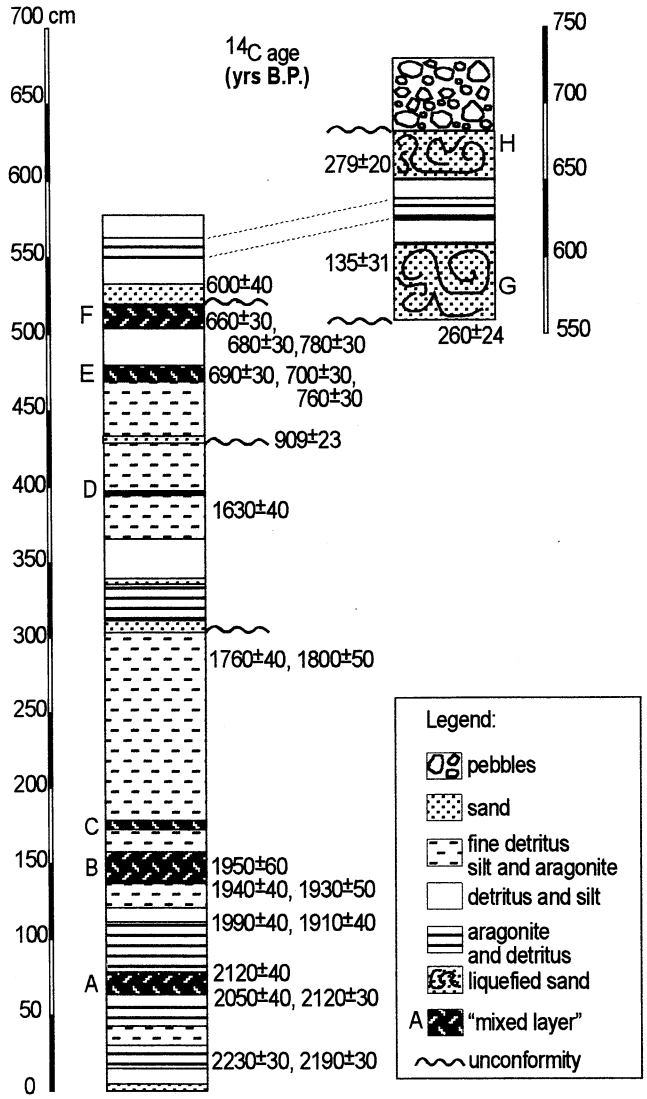

Figure 2. The lithology and chronology of a composite section exposed in Ze'elim Plain. The section is described from two outcrops exposed in different gullies 300 m apart. The correlation between the outcrops is based on the sedimentary sequence, laminae counting, and ^{14}C dates. Ages presented in ^{14}C years B.P. Deformed units (mixed layers and liquefied sands) are marked by capital letters.

the lake during rainy seasons. Well-sorted carbonate silty sand occurs in ripple marks or forms massive beds that were deposited in the nearshore environment. Aragonite crusts covering coarse carbonate sand or lacustrine clay and silt indicate that the deposits were exposed above lake-level at the shore environment. The presence of alluvial sediments (pebbles) indicates relatively low lake level and shifting of the shoreline to the east. The section is disturbed by several unconformities, representing periods of lowering of the lake-level and erosion.

3. Chronology of the Ze'elim Section

The chronology of the Ze'elim composite section is established by 24 radiocarbon ages on vegetation debris (Table 1). The detrital sediments from which the samples were recovered are rich in leaves, stalks, small branches, and seeds that were flushed into the lake with the seasonal floods and buried within the detrital units. The transport time of the analyzed material is probably very short [*Ely et al.*, 1992]. Samples collected in recent fluvial channels in the Dead Sea area yield very high percent of modern carbon (PMC) values, indicating short residence time (< 100 years) of the organic material in the channels [*Yechieli*, 1993].

In most cases, the radiocarbon ages are stratigraphically consistent (Figure 3A). The ages range from 390 B.C. to 1960 A.D.. Radiocarbon analyses of samples from the same stratigraphic horizons yield very similar ages (Table 1). The chronology is discussed further in the context of the ages of the seismic events.

The sedimentation rates vary along the section, ranging from 3 to 13 mm yr^{-1}. In most of the section the sedimentation rate is significantly higher than the average rate in the late Pleistocene Lisan Formation (~0.8 mm yr^{-1} [*Schramm et al.*, 2000]). The higher rate in Ze'elim section reflects the proximity of the section to the Ze'elim Wadi fan-delta. Nevertheless, the Ze'elim section also contains several depositional hiatuses, which lower the average sedimentation rate (Figure 3B).

4. "Mixed layers": Soft Sediment Deformation Structures

The typical sequence of alternating aragonite and detritus laminae and thicker clastic units in the Ze'elim Terrace is interrupted by units that show evidence for soft sediment deformation (Figure 2). These deformed units typically consist of mixtures of fine-grained dark clay and silt, with tabular fragments of aragonite laminae (millimeters to centimeters long) (Plate 1b). The units are a few centimeters to about 20 cm thick, with sharp and flat upper contacts. Below and above each deformed unit the section is laminated and undisturbed. The lateral distribution of the deformed units is not uniform; several of them extend over a large distance and can be traced and correlated among exposures in different gullies and different facies, whereas some have limited distribution.

The origin of the deformed layers is intriguing in light of the flat topography of the Ze'elim Terrace. There is no obvious reason and no field evidence for gravitational slides. Furthermore, the aragonite laminae fragments within the disturbed units are scattered randomly in the dark detritus and show no lateral grading, imbrication or other transport indicators and do not point to any oriented movement as slides or floods over the lake floor. More significantly, the disturbed units extend across sedimentary facies (lacustrine to shore facies) and show no evidence for turbidity currents or any other lateral flow.

Similar layers of fine detritus and tabular aragonite fragments in the Dead Sea basin sediments have been described in the Lisan Formation [*Marco and Agnon*, 1995; *Marco et al.*, 1996]. The disturbed units (termed "mixed layers") were interpreted as seismites largely because of their association with syndepositional surface fault ruptures. It was suggested that each mixed layer represents an originally flat laminated aragonite and detritus unit, which, during an earthquake, was fluidized, brecciated, suspended, and then resettled in its present structure at the water-sediment interface. The flat upper surface of each mixed layer and the undisturbed postseismic layers above them (Plate 1b) point to deformation on the surface of the lake floor during the earthquake events [*Marco and Ag-*

b

a

c

Table 1. AMS Results of Radiocarbon Dating

Laboratory Sample	Height in Section, cm	Dated Material	Radiocarbon Years B.P.	Calibrated Date (2σ)[a]	Most Probable Calibrated Ages
KIA8260 [b]	650 [c]	macro residue, alkali residue	279 ± 20	1520-1670 A.D.	20th century
KIA8261 [b]	600 [c]	wood bark, alkali residue	135 ± 31	1670-1960 A.D.	19th century
KIA8259	550 [c]	Wood, alkali residue	260 ± 24	1520-1800 A.D.	1520-1800 A.D.
KIA3213	478.5-532.5	wood, alkali residue	600 ± 40	1290-1420 A.D.	1290-1420 A.D.
KIA3214A [b]	519	wood twig, alkali residue	780 ± 30	1210-1290 A.D.	1270-1400 A.D.
KIA3215[b]	519	twigs, alkali residue	660 ± 30	1280-1400 A.D.	
KIA3216 [b]	519	plant remains, seed, alkali residue	680 ± 30	1270-1400 A.D.	
KIA3217 [b]	469.5	wood, alkali residue	690 ± 30	1270-1390 A.D.	1220-1390 A.D.
KIA3218 [b]	469.5	wood, alkali residue	700 ± 30	1260-1390 A.D.	
KIA3219 [b]	469.5	wood, alkali residue	760 ± 30	1220-1295 A.D.	
KIA8258	430 [c]	wood, alkali residue	909 ± 23	1030-1210 A.D.	1030-1210 A.D.
KIA3220	381.5	wood, alkali residue	1630 ± 40	340-540 A.D.	340-540 A.D.
KIA3221	282.5	stick, alkali residue	1760 ± 40	130-390 A.D.	130 -390 A.D.
KIA3222	282.5	stem, alkali residue	1800 ± 50	80-390 A.D.	
KIA3223 [b]	146	plant, stem, alkali residue	1950 ± 60	100 B.C. to 230 A.D.	50 B.C. to 230 A.D.
KIA3224	132.5	wood, alkali residue	1940 ± 40	50 B.C. to 140 A.D.	50 B.C. to 180 A.D.
KIA3225	132.5	wood, alkali residue	1930 ± 50	50 B.C. to 220 A.D.	
KIA3227A	107	diverse plant mater., alkali resid.	1990 ± 40	50 B.C to 80 A.D.	50 B.C. to 80 A.D.
KIA3227B	107	diverse plant material, humic acid	1910 ± 40	0-230 A.D.	
KIA3228 [b]	73.5	diverse plant mater., alkali resid.	2120 ± 40	360 -40 B.C.	200-40 B.C.
KIA3232	51	root or twig, stem, alkali residue[d]	2050 ± 40	170 B.C. to 50 A.D.	200 B.C. to 10 A.D.
KIA3233	51	wood, alkali residue	2120 ± 30	350 -40 B.C.	
KIA3234	14.5	stem and root, alkali residue[d]	2230 ± 30	390 -200 B.C.	380-180 B.C.
KIA3235	14.5	stem, alkali residue	2190 ± 30	380 -160 B.C.	

[a] Calibrated ages (2σ) according to *Stuiver et al.* [1998]. The samples are listed according to their stratigraphic height, top to bottom.
[b] Samples collected from the deformed units.
[c] Samples collected from the southern section (see composite section, Figure 2).
[d] Root debris (not in situ root).

non, 1995, Figure 4]. The deformation occurred prior to the deposition above. Irregular surfaces of the mixed layers are observed locally, where they overlie syndepositional fault ruptures. In this places subaqueous scarps were created during the seismic event [*Marco and Agnon,* 1995]. Similar soft sediment deformation structures have been documented in several other localities worldwide and also interpreted as seismites [cf. *Allen*, 1986; *Davenport and Ringrose*, 1987; *Hempton and Dewey*, 1983; *Sims*, 1973, 1975]. For example, *Doig* [1991] describes a chaotic zone of organic-rich lake sediment mixed with partly tabular fragments of a previously laminated silt layer that was disturbed during the 1935 (*M*6.3) Témiscaming (Quebec) earthquake.

5. Distribution of Deformation in Different Depositional Environments

The sediments exposed at the Ze'elim Plain were deposited in a transition zone between two depositional environments of a lacustrine basin: the shore and near-shore environment and the lake water body. This setting is ideal for the purpose of analyzing the effects of simultaneous ground shaking on sediments with different properties (e.g., aragonite–detrital laminae versus sandy units) because it is possible to trace continuously the changes in deformation character along with the facies variations. Where the lacustrine lithology changes to silt and sorted sand of the shore environment, load-cast and flame

Plate 1. (a) The Late Holocene outcrop exposed at the Ze'elim Plain, viewed from the lake shore to the west. The western escarpment of the Dead Sea Graben is seen in the backside. The Ze'elim Plain was covered by the Dead Sea 15-20 years ago. A drastic retreat in the lake level (~80 cm y^{-1}) incised deep gullies and exposed the sediments of the upper Ze'elim Formation. The present thickness of the exposed section reaches about 7 m. (b) Mixed layer B (see also Figure 2) composed of aragonite fragments suspended in fine dark detritus. The fragments are few millimeters to few centimeters long and do not show any preferred orientation. The overlying and underlying (not seen in the figure) laminated deposits are undisturbed. This layer is correlated with the 31 B.C. earthquake (see text). (c) Liquefied carbonate sands, fine detritus, and aragonite laminae of the shore environment. This deformed unit (~ 0.5 m thick) illustrates the simultaneous deformation of deposits from different depositional environments in the same stratigraphic horizon, which was at the surface at that time.

structures are visible (Plate 1c). The thickness of the deformed unit changes within a short distance. It is clearly visible that the character of deformation is related to grain size and the thickness of the unit. When the sand units become too thin, the deformation disappears.

The change in the deformation pattern is illustrated here by the behavior of a prominent mixed layer (B in Figure 2). This mixed layer can be traced over the entire studied area, across the facies changes. Yet it exhibits different structures according to the type of the sediments.

The observation of simultaneous deformation in different sedimentary facies of the same stratigraphic horizon in Ze'elim outcrops, supports the interpretation of the mixed layers as seismites. No other process could have simultaneously affected the various depositional environments of the same stratigraphic horizon. Together with the juxtaposition of the mixed layers over surface ruptures (as observed in the Lisan Formation), the transformation of disturbance through various sedimentary facies strongly supports the interpretation of the mixed layers as seismites.

6. Dating and Correlation of the Seismites With Historic Earthquake

The ages of the deformed layers were constrained by ^{14}C dates derived from the layers themselves and by extrapolating

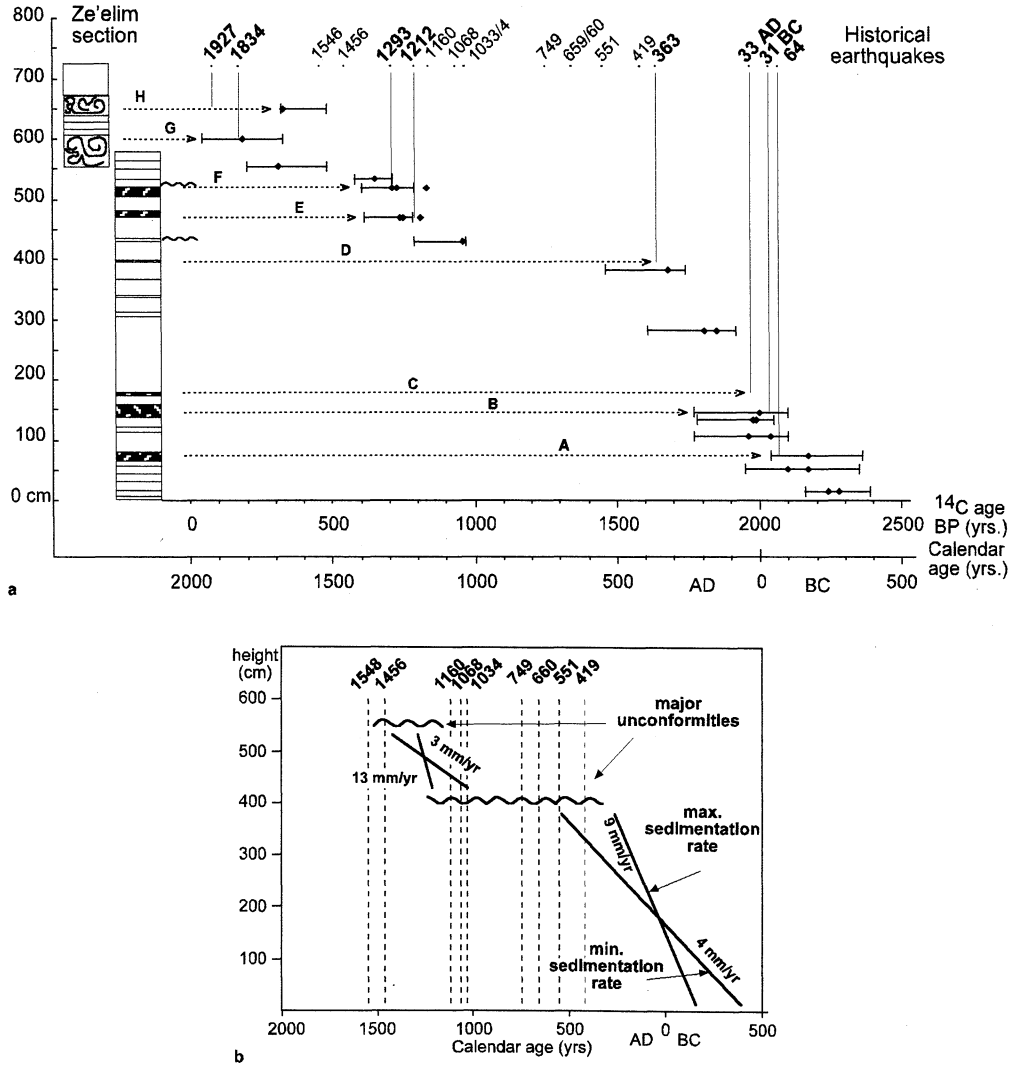

Figure 3. (a) Chronology of the deformed units (seismites) in the Ze'elim section. Solid dots represent ^{14}C ages in years B.P.. Error bars represent the ranges in the calibrated ages (2σ) of all samples in each stratigraphic horizon. Vertical thin lines represent historical earthquakes in the Dead Sea area, which were correlated to the deformed units in the Ze'elim section. Horizontal dashed arrows are drawn from the deformed units (listed in capital letters) to the correlative earthquakes. (b) Sedimentation rates calculated for the lower part of the composite section. The longest calibrated range was used for calculating the minimum sedimentation rate, and the shortest range for calculating the maximum sedimentation rate. Two clear unconformities are evident: The upper one is dated to 1290-1420 A.D, and the lower one to 1030-1210 A.D.. The lower unconformity is marked by a sharp decrease in the sedimentation rate. Vertical dashed lines represent earthquakes that lie within the sedimentological hiatuses. Sedimentation rate of the upper part in the section was not calculated because datable samples were insufficient.

Table 2. The ^{14}C Chronology of the Deformed Layers (Seismites)

Deformed Layer [a]	Sample Laboratory Number	Calendar Age Years (2σ)	Most Probable Calibrated Ages
A	KIA3228	360-40 B.C.	200 -40 B.C.
B	KIA3223	100 B.C. to 230 A.D.	50 B.C. to 230 A.D.
C	-	64 B.C. to 311 A.D.[b]	5 -50 A.D.
D	-	358-580 A.D.[b]	358-580 A.D.
E	KIA3219, KIA3218, KIA3217	1220-1390 A.D.	1220 -1390 A.D.
F	KIA3214A, KIA3215, KIA3216	1270-1400 A.D.	1270 -1400 A.D.
G	KIA8261	1670-1960 A.D.	19th century
H	KIA8260	1520-1670 A.D.	20th century

[a] Listed by their stratigraphic height, bottom to top.
[b] Age calculated according to sedimentation rate, interpolated from adjacent dated layers.

between ages of layers directly beneath and above a particular mixed layer (Table 2). The radiocarbon ages of the mixed layers were calibrated to calendar years according to *Stuiver et al.* [1998]. The calibrated ages lie in ranges that are defined by the 2σ envelope error of the measured data. For example, the measured radiocarbon age of event A (2120±40 years B.P., Table 1) is calibrated to the range of 360 to 40 years B.C.. Applying the superposition principle and rate of sedimentation further narrowed these ranges. Samples, which are stratigraphically lower in the section, thus older, reduce the calendar range of the samples above. This procedure allows us to resolve the calendar ages of samples that yielded analytical data that are statistically indistinguishable. The use of sedimentation rates allows determining ages of mixed layers that were not directly dated by radiocarbon because of lack of organic debris. The sedimentation rate is sensitive to depositional hiatuses in the section. Thus, different rates are used for different parts of the section (see varying slopes in Figure 3b).

The radiocarbon sample collected from a mixed layer is dating the deposition within the layer before it was disturbed. Hence the seismic event that caused the deformation is younger. The time elapsed between the deposition and the deformation by the earthquake was short relatively to the uncertainty in the dating. Two lines of evidence support this assumption:

1. Deformation of the mixed layer occurred at the sediment-water interface. This is indicated by graded bedding and by the juxtaposition of mixed layers with syndepositional faults in the Lisan Formation. Thicker accumulation above the mixed layer on the downthrown block is considered as evidence for a fault scarp. Some local mass transport near the scarp produced thicker mixed layers in the lower block [*Marco and Agnon*, 1995].

2. In the Ze'elim section, two of the mixed layers, A and B, are separated by only about 75 cm and approximately 200 ^{14}C years (Figure 2). Thus, the time elapsed between the deposition and disturbance of unit A must have been shorter than 200 years.

Liquefaction is often attributed to subsurface deformation. In Ze'elin section liquefaction seems to have occurred at the surface. This surface deformation is consistent with the absence of sand volcanoes and dikes.

A final assessment of the mixed layer ages and their identification as seismites is achieved by correlation with the chronology of the historical earthquakes. The concept we used here is to assess whether all individual pieces of information (the structures, the ages and the correlation to known chronology) fit an internally consistent framework.

6.1. Comparison With the Historical Earthquake Record

The historical earthquake record of the last four millennia in the Middle East [*Ben-Menahem*, 1991] represents one of the longest seismic records on Earth. The dated paleoseismic record recovered from the mixed layers in the Ze'elim Terrace correlates with the last and best documented 2000 years of this record (see description of the relevant historical earthquakes in Table 3). Several reported historical earthquakes are not identified in the Ze'elim record but can be correlated with depositional hiatuses or periods of erosion. Conversely, it is possible to correlate all deformed units with particular historic earthquakes.

The correlation between the Ze'elim seismic record and the historical record is based mainly on reports from three sites in the Dead Sea region: Jericho, Karak, and the Darga fan delta (Figure 4). Jericho is located to the northwest of the Dead Sea adjacent to one of the major faults, the Jericho Fault (Figure 1) [*Reches and hoexter*, 1981]. The site was settled in the Neolithic period and has been continuously populated during the time represented by the Ze'elim section. Karak is located on the eastern escarpment of the Dead Sea Graben, 1400 m above the Dead Sea shore. Its prominence peaked during the Crusaders period, and it has been populated continuously during the last millennium. We also compare our data to the Darga fan delta (Figure 1), where a geological earthquake record was recently described [*Enzel et al.*, 2000]. The historical and geologic reports on earthquakes around the Dead Sea area are summarized in Figures 4 and 5.The following events are identified in the Ze'elim section:

6.1.1. Event A. Event A was dated based on a mixed layer sample collected 73.5 cm above the bottom of the section. The age of the sample is 2120±40 radiocarbon years B.P. (Table 1), with a calibration range of 360-40 B.C.. Below this mixed layer, at 14.5 cm, two samples were dated to 2190±30 and 2230±30 years B.P. (with calibration ranges of 380-160 B.C. and 390-200 B.C., respectively). At 51 cm, two other samples were dated to 2120±30 and 2050±40 years B.P. (350-40 B.C. and 170 B.C.-50 A.D., respectively). Taken together, the four samples constrain the age of event A within the calendar range of 200 B.C.-40 B.C..

Mixed layer A, which is the oldest in the section, can be correlated to the historically documented 64 B.C. earthquake, which was felt strongly in Jerusalem and damaged the city walls and the Second Temple [*Amiran et al.*, 1994]. A deformed unit in the Darga fan delta was also dated to this time range [*Enzel et al.*, 2000]. The appearance of deformed units in both the Ze'elim Terrace and the Darga fan delta during the 64 B.C. earthquake may indicate that the epicenter was located

Table 3. Description of Earthquakes in the Dead Sea Region According to Historical Reports

Date	Location and Description	References
64 B.C.	In Jerusalem the Temple and city walls were damaged. In Syria it was felt as far as Antioch.	1,7
31 B.C.	Reports were from Israel. There was great destruction in the Dead Sea area (e.g. Herod's winter palace in Jericho, Qumran and Massada). Severe damage occurred in the Galilee, and Judea. In Jerusalem the earthquake damaged the Second Temple. According to Josephus, 30,000 people were killed.	1,5,7,8
	Epicentral intensity was possibly MMS X.	
33 A.D.	Reports were from Judea region. The Temple in Jerusalem was damaged.	1,7
363 A.D.	Reports were from Baniyas in the north through Petra in the south and from the coastal littoral through the Jordan Valley and beyond. In Jerusalem the Temple area was damaged. In Syria several castles were damaged. Karak was destroyed. Seiche was reported in the Dead Sea.	1,3,4,5,7,8
419 A.D.	In the reports, Jerusalem is specifically mentioned. Many towns and villages were destroyed (e.g., Aphek/Antipatris). The shock was moderate to severe.	1,4,7,8
551 A.D.	Reports were from northeast Egypt (?), Israel, Arabia, Phoenicia, Syria, and north Mesopotomia. Damage was reported along the Lebanon coast and in villages in the Galilee. Damage occurred in Jerusalem, Jerash, Mount. Nebo. The el-Lejjun fortress east of Karak was destroyed. Petra was destroyed and never rebuilt. Tsunami occurred on the coast of Lebanon.	1,4,7
	There are different suggested epicenter locations: offshore from Lebanon or in the Jordan Valley.	
659/660 A.D.	Reports were from Jordan Valley and Rehov in Beth Shean basin. In Jericho it was felt strongly. The monasteries of St. John the Baptist (on the Jordan river, east of Jericho) and St. Euthymius were destroyed.	4,7,8
749 A.D.	Reports were from Egypt, Mesopotamia, Syria, Arabia, and Israel.	4,5,6,7,8
	Damage occurred to 600 settlements, and there were many casualties on both sides of the Jordan, from Tiberias to Arad. Hisham Palace near Jericho and buildings in all major cities and monasteries were destroyed. A Seiche was reported in Lake Galilee and the Dead Sea. Tsunami occurred on Mediterranean coast.	
	Epicentral intensity possibly MMS X. Local magnitude was estimated to 7.3.	
1033/1034 A.D.	Reports were from Syria, along the Jordan Valley, as far has Gaza and Ashkelon and probably in the Negev and Egypt. Heavy damage and casualties occurred in Tiberias. The earthquake affected the Galilee, Akko, Jaffa, Nablus, Ramle, Jerusalem, Hebron, and Jericho. Tsunami occurred on the Mediterranean coast of Israel.	2,5,6,7
	Epicentral intensity possibly MMS X. Suggested epicenter near the Lake of Galilee.	
1068 A.D.	Reports were from northwest Arabia. The city of Elat was completely ruined, and its inhabitants perished. In Tabuk, new springs appeared. The earthquake was felt at Wadi al-Qura, Khaibar, and al-Marwa and as far as Medina, Yanbu, and Badr in the south. In the Baniyas, 100 people died under the debris. Ramla was destroyed, and 15,000 people died (seems exaggerated). In Jerusalem the roof of the Dome of the rock was displaced. Yavne and Ashdod were affected. Tsunami washed Israel coast.	2,6,7
	The epicentral area of this earthquake must be sought in the sparsely inhabited region between Elat and Taima in Northern Hejaz.	
1160 A.D.	Reports were from Israel alone. Slight damage occurred in Bethlehem and Jerusalem. The Monastery of Mar Elias (Jerusalem) was seriously damaged and the Monastery of St. John on the Jordan River was destroyed	1,7
1212 A.D.	Reports were from south Israel and Egypt. It was strongly felt in Cairo and Fustat, and destroyed a number of houses. At al-Shaubak and Karak (VIII MMS) towers and houses were destroyed, killing a number of women and children. Strong in Elat (VIII-IX MMS). In Sinai Peninsula the shock caused severe damage to the monastery of St. Catherine. The earthquake was located in the gulf of Aqaba or south of the Dead Sea.	6,7
1293 A.D.	Most of the reports come from south and central Israel. The earthquake damaged Gaza (VII MMS) Ramla (VII MMS), Ludd (VI MMS), Qaqun, and Karak (VIII MMS), where three fortress towers destroyed. The earthquake ruined many places on the coast of Israel. The epicenter was probably in the Dead Sea Rift.	2,6,7
1456-1459 A.D.	Reports were from southern Israel and Jerusalem. It was felt weakly in Cairo. In Karak, destruction and casualties are reported.	1,6,7
1546 AD	Damage and victims were reported from Safed, Tiberias, Ramla, Jerusalem, Hebron, Gaza, Salt, and Karak. In Nablus hundreds of victims were buried under the ruins. The earthquake was felt as far as Damascus. The flow of the Jordan River was stopped for 2 days by a landslide near Damia. Tsunami washed the Mediterranean coast from Jaffa to Gaza. Seiche occurred in the Dead Sea.	1,5,6,7
	Maximum epicentral intensity was MMS IX.	
1834 A.D.	Damage reports were from Jerusalem, Bethlehem, Nablus, Gaza, and Karak. It was felt strongly in Tiberias, Akko, and Ashkelon. Large blocks of asphalt floated on the Dead Sea. The shallow	1,5,7

Table 3. (continued)

Date	Location and Description	References
	water road connecting the Lisan with En-Gedi disappeared, and the Dead Sea became impassable by foot.	
1927 AD	Reports of great damage were in Judea and Samaria in Israel. The flow of the Jordan River stopped for 22 hours due to landslides near Damia. The earthquake was felt in Syria and Lebanon. This is the first major earthquake in the area to be recorded instrumentally. M=6.25, maximum epicentral intensity was MMS IX in the Jordan Valley. Revised epicenter was located near Darga fan-delta on the shores of the Dead Sea. Sites far from the epicenter such as Nablus, Ramla, and Lod also experienced relatively high local intensity (MMS VIII). On the other hand, the towns closer to the epicenter, i.e., Jericho and Jerusalem, experienced lower intensity (MMS VII).	9,10,11,12

The information is collected from historical catalogues. The catalogues summarize information from different historical sources that were studied and analyzed during the last century. Our assessment is based on the information that is written in the catalogues only. References are 1, *Willis* [1928]; 2, *Arieh* [1977]; 3, *Russell* [1980]; 4, *Russell* [1985]; 5, [*Ben-Menahem* [1991]; 6, *Ambraseys et al.* [1994]; 7, *Amiran et al.* [1994]; 8, *Guidoboni et al.*, [1994]; 9, *Ben-Menahem et al.* [1976]; 10, *Vered and Striem* [1976]; 11, *Shapira et al.* [1993]; 12, *Avni* [1999]. All references are based on historic sources that are described therein.

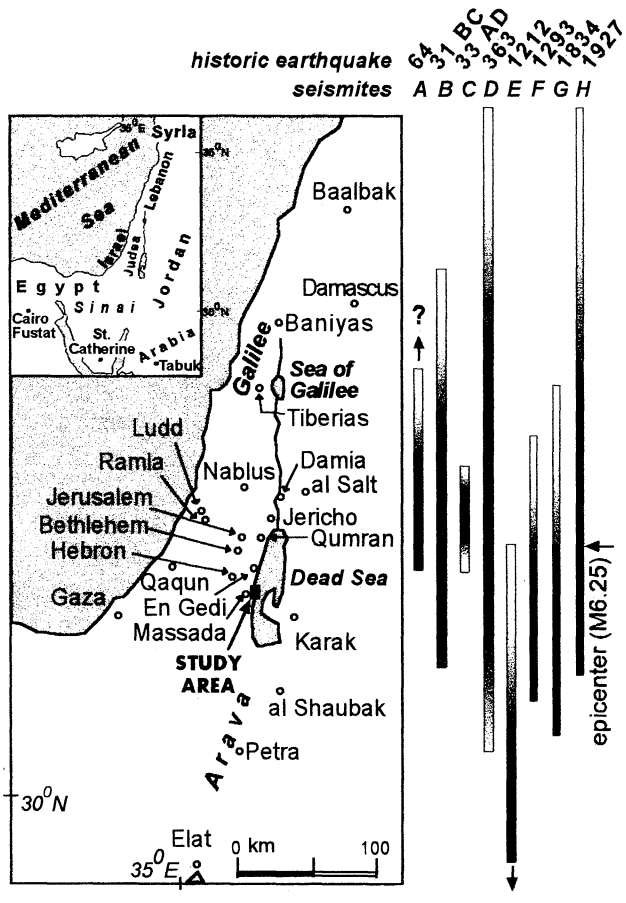

Figure 4. Location map of sites that were affected by earthquakes generated in the Dead Sea area (see Table 3 for historical information and references). On the right side, the area affected by the earthquakes according to the historic reports and the new evidence from this study. Estimated epicenter locations along the Dead Sea fault system are indicated by the gradual change into darker shading. The 1927 A.D. earthquake is likely better represented by the historical data relatively to older events mainly because it is a recent event.

in the Dead Sea area (Figure 5). The lack of independent reports from other places in the area probably reflects the event's antiquity and moderate intensity.

6.1.2. Event B. The time elapsed between events A and B was bracketed by four radiocarbon dates: 1910±40 and 1990±40 years B.P. (0 to 230 A.D., 50 B.C. to 80 A.D.) for samples at 107 cm, and 1930±50 and 1940±40 years B.P. (50 B.C. to 220 A.D. and 50 B.C. to 140 A.D., respectively) for samples at 132.5 cm. Based on the age of a sample collected from within the mixed layer itself at 146 cm event B was dated to 1950±60 years BP (100 B.C.-230 A.D.), a range which overlaps with that of the samples between events A and B. Nevertheless, the age range of event B can be reduced to 50 B.C. to 230 A.D. according to its statigraphical location above event A. Moreover, the association of event A with the 64 B.C. earthquake implies that event B is younger and may be correlated with an earthquake that took place in the early spring of 31 B.C..

The 31 B.C. earthquake is described by Josephus Flavius in the "Jewish Wars" (Book I, Ch. XIX, 370-380) and in "Jewish Antiquities" (Book XV, Chapter. V, pp. 121-147). The earthquake occurred during the battle of Actium between Caesar and Anthony in the seventh year of King Herod's reign. According to Flavius, the earthquake caused great destruction and many casualties, killing as many as 30,000 people. The Second Temple in Jerusalem, Herod's winter palace at Jericho, and structures in Massada and Qumran were damaged [*Amiran et al.*, 1994; *Ben-Menahem*, 1991; *Guidoboni et al.*, 1994]. The earthquake was strongly felt in Judea and the Galilee (Figure 4).

The mixed layer of event B can be traced along all the outcrops in the study area and can also be identified in the Darga fan delta [*Enzel et al.*, 2000]. On the Jericho Fault, a surface rupture that has also been related to the 31 B.C. earthquake [*Reches and Hoexter*, 1981] is located near the city of Jericho, about 60 km north of the Ze'elim Terrace (Figure 1). Local intensity is inferred to have reached MMS X in several places [*Amiran et al.*, 1994]. Considering the geological evidence and trusting the extensive historical records, despite their antiquity, it can be concluded that the 31 B.C. event was a strong earthquake with an epicenter located on the main Jericho Fault, not far from the Ze'elim Terrace.

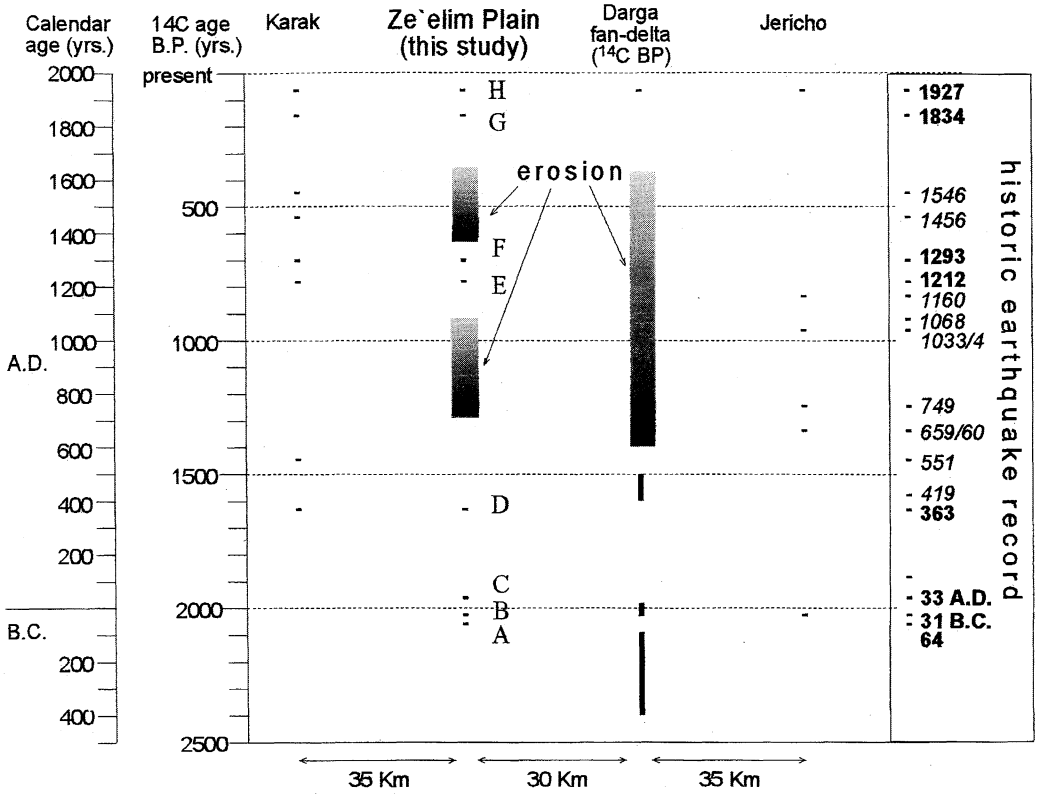

Figure 5. The historical record of earthquakes that have been reported to affect the Dead Sea area during the Late Holocene. The Ze'elim Terrace (this study) and the Darga fan delta [*Enzel et al.*, 2000] are geological records. The Karak and Jericho records are composed of the historical reports of damage from these sites. At the right column the complete historic earthquakes record is presented (Table 3). The criterion of choosing an earthquake to be presented in the historical record is that there are distinct reports of damage in the Dead Sea area or Jerusalem (which was occupied during the entire historical record presented). Bold indicates historical earthquakes recovered from the Ze'elim Terrace. Italics indicates earthquakes that are reported in the historical record but do not appear in the Ze'elim section (see text). Capital letters indicate the corresponding deformed unit in Ze'elim Terrace.

The prominent thickness and regional distribution of mixed layer B further argue that it can be identified with the 31 B.C. earthquake. We will subsequently use this mixed layer as a chronological "anchor point", which is used in the assessment of the ages of other mixed layers.

6.1.3. Event C. Mixed layer C is a few cm thick and discontinuous. It is located at 178.5 cm, 32.5 cm above the sample that dates the previous event (at 146 cm). Since no organic debris was found in unit C, the event was dated according to the sedimentation rate at this part of the section (4-9 mmy $^{-1}$, Figure 3b) to a calendar range of 64 B.C. to 311 A.D.. This range can be further reduced to 5-50 A.D. by using the 31 B.C. earthquake (event B) as a chronological anchor point in the section. Mixed layer C is correlated with the earthquake of 33 A.D. that damaged the Second Temple in Jerusalem [*Amiran et al.*, 1994; *Willis*, 1928]. The earthquake was not reported elsewhere in the Dead Sea area. The lack of documentation and the limited evidence for geological disturbance suggest a small magnitude earthquake in the Dead Sea area (Figure 4).

6.1.4. Event D. Mixed layer D contains no organic debris for radiocarbon dating, therefore the age of this event was estimated from the sedimentation rate in the underlying interval. The samples below and above mixed layer D were dated to 1630±40 years B.P. (340-540 A.D.) and 909±23 years B.P. (1030-1210 A.D.), respectively. The older sample was located at 381.5 cm and the younger at 430 cm from the bottom, yielding a sedimentation rate of 0.5-1 mm y^{-1}. This rate probably represents a minimum value because the younger sample was collected above a depositional unconformity. The unconformity is characterized by coarse sand and aragonite crusts that indicate lowering of the lake level, which is usually accompanied by erosion of the surface. The erosion is probably the reason for the low sedimentation rate (e.g. an order of magnitude lower than the one in the previously studied interval). Therefore, for the interval including layer D we assign the mean sedimentation rate that characterizes the lower part of the section (4-9 mm y^{-1}, Figure 3b). This rate would yield a calibrated age for event D in the range of 358-580 A.D.. A similar result is achieved when the 31 B.C. earthquake (top of unit B) is taken as a chronological anchor point in the section. Mixed layer D was probably deformed by the 363 A.D. earthquake. Documentary evidence concerning this earthquake is preserved in a letter originally composed and circulated in Cyril's name (the Bishop of Jerusalem) during the early years of the 5th century [*Russell*, 1980]. The destruction caused by

this earthquake stretched from Baniyas in northern Israel through Petra and Elat in the south and from the Mediterranean coast through the Jordan Valley and eastward [*Russell*, 1985]. Damage in Karak and a seiche in the Dead Sea in response to the earthquake are reported [*Amiran et al.*, 1994]. In the Darga fan delta, a liquefied unit [*Enzel et al.*, 2000] is probably associated with the same event.

6.1.5. Events E and F. The timing of event E is inferred from the ages of three samples from this mixed layer: 760±30, 700±30, and 690±30 years B.P.. Event F is dated by three samples from the next mixed layer to 780±30, 680±30, and 660±30 years B.P.. The 780 years B.P. sample (within unit F) is out of stratigraphic order and probably represents reworked material; thus it is excluded from the analysis. The calibrated ranges for E and F are 1220-1390 A.D. and 1270-1400 A.D., respectively. Statistically, these dates are indistinguishable, but their stratigraphic order suggests a correlation to the earthquakes of 1212 and 1293 A.D.. The two mixed layers are separated by a 20-30 cm thick uniform detrital unit that represents approximately 20-100 years of deposition, based on the sedimentation rate in this part of the section (3-13 mm y^{-1}, Figure 3b). The calculated age difference between the two mixed layers is similar to the historical age interval between the two earthquakes.

The 1212 A.D. earthquake was strongly felt in Egypt, particularly in Cairo and Fustat. At al-Shaubak and Karak, towers and houses were destroyed, and casualties were reported. In the Sinai Peninsula, the shock caused severe damage to the monastery of St. Catherine [*Ambraseys et al.*, 1994]. Based on the distribution of damage, it was suggested that the earthquake's epicenter must have been located south of the Dead Sea [*Ambraseys et al.*, 1994] (Figure 4).

The epicenter of the 1293 A.D. earthquake was probably located in the Dead Sea basin near Karak, [*Arieh*, 1977]. This earthquake affected the region of Gaza, Ramla, Ludd, Qaqun and Karak, where towers and many houses were destroyed [*Ambraseys et al.*, 1994]. The 1293 A.D. as well as 1212 A.D. earthquakes where not reported from Jericho suggesting that their epicenters may be located south to the Dead Sea basin (Figure 4).

6.1.6. Events G and H. These events are recorded as liquefied sand layers in the uppermost part of the Ze'elim section (Figure 2). Thus, they may record the youngest reported earthquakes in the region, probably from the last two centuries. The most pronounced and well-documented earthquakes of that period are those of 1834 and 1927.

Events G and H are constrained by radiocarbon ages from three samples, which are arranged in the following stratigraphic order from bottom to top: 260±24, 135±31 and 279±20 years B.P.. These correspond to calibrated ranges of 1520-1800 A.D., 1670-1960 A.D. and 1520-1670 A.D., respectively (Figure 3a). In addition, the liquefied layers G and H are separated by a few centimeters of lacustrine sediments (laminated aragonite and detritus), which mark a rise in lake level and may be related to the relatively high stand of the Dead Sea at the end of the 19 th century [*Klein*, 1961]. It appears that the lower and middle layers are older than the 1890's lake level rise and the upper layer (H) is younger. The range of ages of the middle and lower layers is consistent with this interpretation, while that of the upper layer is out of the stratigraphic order and inconsistent with the 1890's high-stand. The discrepancy could reflect reworking of the organic debris, which occurs in the shore environment. If the lacustrine layer corresponds to the 1890's high-stand, then the upper liquefied layer H can be correlated with the 1927 earthquake and layer G with the previous 1834 event. The identification of mixed layer H with the 1927 earthquake indicates that water depth was ~10 m above the deformed sediment (the Dead Sea elevation during 1927 was 392 mbsl [*Klein*, 1982] and the deformed unit is at about 402 mbsl).

Accounts of damage from the 1834 A.D. earthquake are reported from Jerusalem, where several churches and minarets and the city wall were damaged. At Bethlehem, several monasteries were damaged and many people were killed [*Amiran et al.*, 1994]. Nablus and Gaza were also damaged. Large blocks of asphalt appeared on the Dead Sea [*Ben-Menahem*, 1991]. This earthquake damaged Karak, but it is neither visible in the Darga fan delta section nor reported to have damaged Jericho (Figure 5). Therefore, the epicenter was likely south of the Dead Sea basin (Figure 4).

The 1927 earthquake is the only relatively large (M=6.25) earthquake in Israel to be recorded instrumentally [*Ben-Menahem et al.*, 1976]. Its epicenter was reinterpreted recently to have been located just north of the Darga fan-delta (Figure 1) [*Shapira et al.*, 1993]. Evaluations of the effects of this earthquake yield a maximum intensity MMS IX along the Jordan River, from the Allenby Bridge (south east of Jericho) southward to the north coast of the Dead Sea [*Avni*, 1999]. The 1927 earthquake was correlated with the youngest deformed layer in Darga fan-delta [*Enzel et al.*, 2000].

6.2. Reported Historic Earthquakes That Are Not Visible in the Geological Record

Several earthquakes from the Dead Sea area that are reported in the historical catalogues have no correlative deformed units in the Ze'elim record (Figures 3b and 5). The absence of these earthquakes from the Ze'elim record may be due to a remote epicenter and or small magnitude (<5.5), which was not sufficient to induce a disturbance in the Dead Sea area. Another obvious reason is the incompleteness of the geological record in the Ze'elim Terrace. During times of climatic change, the lake level dropped and the Ze'elim Terrace was exposed, resulting in depositional hiatuses.

Two major unconformities are identified in the section (Figures 3b and 5). To constrain the ages of the hiatuses we determined three ranges of calibrated ages for each unconformity. The first range is obtained from the closest samples below an unconformity; the second range represents samples obviously related to the unconformity (samples recovered from sand and aragonite crust); the third range is of samples collected from layers above the unconformity. The older unconformity has yielded the respective ranges of 340–540 A.D., 1030–1210 A.D. and 1220-1390 A.D. (Table 1). The younger unconformity has yielded the ranges 1270–1400 A.D., 1290-1420 A.D., and, 1520-1800 A.D. (Table 1). The age ranges presented in Figure 3 are the samples obviously related to the unconformities (i.e. the second age range).

Nine earthquakes reported in historical documentation from the Dead Sea area do not appear in the Ze'elim seismite record and they all fall in the unconformities and depositional hiatuses discovered in the section (Figure 3b). This is consistent with the interpretation of the mixed layers as earthquake induced structures in the Ze'elim record. If a strong earthquake that was reported broadly in the Dead Sea area would be

missing from a complete sedimentary record, it would have been difficult to explain the interpretation of the mixed layers as seismites.

The 419, 551, 659/660, 749, 1033/1034, 1068, 1160 A.D. dates are correlative to the first major unconformity and the 1458 and 1546 A.D. earthquakes are correlative to the younger unconformity (description of the earthquakes in Table 3). It is impossible to determine according to the Ze'elim record whether these events were generated in the Dead Sea area. Probably, few of the events were too remote or of moderate magnitude. However, the 749 A.D. earthquake caused regional damage along the Dead Sea Transform, destroyed the Hisham Palace in Jericho, and was identified as a fault rupture on the Jericho Fault [*Ambraseys et al.*, 1994; *Amiran et al.*, 1994; *Ben-Menahem*, 1991; *Guidoboni et al.*, 1994; *Reches and Hoexter*, 1981]. This earthquake probably did affect the Ze'elim area, but the evidence was lost. We predict that this event will be identified in cores taken from deeper parts of the lake, where erosion due to lowering of the lake level is less frequent.

7. Recurrence Intervals of Earthquakes in the Dead Sea Area

The outcrops in the Ze'elim Terrace represent almost the entire last two millennia in the geological history of the Dead Sea region. Combined with the historical record, the evidence from these sediments provides constraints on the temporal and spatial distribution of earthquakes in the region.

In the Ze'elim Terrace eight deformed units have been identified as seismites. These are correlated to historical earthquakes that occurred in 64 and 31 B.C. and in 33, 363, 1212, 1293, 1834, and 1927 A.D.. Other historical earthquakes probably occurred during the two periods of depositional hiatuses. Overall, the deformed units and the historical record indicate that a minimum of 8 to a maximum of 17 earthquakes affected the Dead Sea area within a period of about 2000 years, implying a recurrence interval of about 100-300 years. Based on reported earthquake damage *Ben-Menahem* [1991] estimated that the recurrence time of strong earthquakes (e.g., M=7.3) in the southern half of the Dead Sea Transform is about 1500 years. The significantly shorter recurrence interval estimated from the Ze'elim record probably reflects its sensitivity to a broader range of earthquake magnitudes. The threshold intensity of these earthquakes is largely an unresolved question. We estimate it, however, as M>5.5 at epicentral distances smaller than 100 km, a figure that can accommodate the observation of liquefaction and fluidization in the deformed units of the Ze'elim section. Liquefaction of sand may occur during earthquakes of magnitudes as low as 5 [*Audemard and Santis*, 1991], in most cases liquefaction and fluidization of sediments are associated with earthquakes of magnitude 6 and greater [*Allen*, 1982]. Liquefaction of sediments occurs within the first tens of kilometers from the epicenter [*Ambraseys*, 1988; *Obermeier*, 1996]. At distances exceeding 100 km, M_S = 7 appears to be a minimum threshold for causing liquefaction. Based on this information and the previous estimates from the mixed layers in the Lisan Formation record [*Marco et al.*, 1996], it is reasonable to suppose that the mixed layers observed in the Ze'elim outcrops document the seismicity in the Dead Sea area. The earthquake magnitudes were probably of M>5.5 and the epicenters of the earthquakes that caused them lie within several tens of km from their occurrence.

Reches and Hoexter [1981] estimated a recurrence interval of about 1000 years, based on ruptures on the Jericho Fault (Figure 1). The sediments in the Ze'elim Terrace record more earthquakes for two reasons: (1) Earthquaks that do not rupture the surface may still generate mixed layers. Moreover, even earthquakes that rupture the surface require significant slip for showing in coarse sediments as those trenched by *Reches and Hoexter* [1981]. For example, the maizoseismal zone of the 1927 earthquake indicates rupture on the Jericho Fault [*Avni*, 1999], yet this rupture is not expressed in the trenches of *Reches and Hoexter* [1981]. (2) The sediments in Ze'elim terrace were disturbed by ruptures on various faults in the Dead Sea area, and not only by ruptures on the Jericho Fault. The Ze'elim sediments record a regional and not a fault specific recurrence interval, hence the recurrence interval calculated in this work cannot be compared with recurrence intervals calculated according to specific fault ruptures.

Liquefied layers identified in the Darga fan-delta sequence indicate a recurrence interval of approximately 600 years for earthquakes with M>5.5 [*Enzel et al.*, 2000]. The reconstruction of the Darga fan delta paleoseismic record is similar to that of Ze'elim, although the sediments in Ze'elim are of a more lacustrine nature. The fine laminae and the less and smaller depositional hiatuses and unconformities in the Ze'elim section make the paleoseismic record more sensitive. This may explain why more historical earthquakes are represented in the Ze'elim section and the recurrence period is somewhat shorter.

The temporal distribution of earthquakes was recovered from the ~50000 years paleoseismic record of the late Pleistocene Lisan Formation (in outcrops located a few kilometers west of our study area) [*Marco et al.*, 1996]. The Lisan paleoseismic record indicates that the events cluster at periods of ~10,000 years, separated by quieter periods of similar length. Within the clusters the rate of activity reported by *Marco et al.* [1996] is 8 earthquakes in 5000 years (recurrence interval of 400 years). Comparing the Ze'elim record with the long-term Lisan record suggests that the Dead Sea area has been in an active seismic cycle during the past 2000 years.

8. Location of Epicenters of Paleoearthquakes

The epicenters of the earthquakes that deformed the sediments in Ze'elim Terrace were probably within the Dead Sea basin, not more than a few tens of kilometers from the study area. A surface rupture and an epicenter are more precisely known for only two events recorded in the Ze'elim Terrace, the 31 B.C. event and the 1927 A.D. event, respectively. Both events were generated on the Jericho Fault [*Reches and Hoexter*, 1981; *Shapira et al.*, 1993]. The 31 B.C. earthquake created a distinct mixed layer in the Ze'elim sequence, about 65 km from where the fault rupture was identified in a paleoseismic trench east of Jericho [*Reches and Hoexter*, 1981]. In the Darga fan-delta, the event is marked by very large slump structures located above the Jericho Fault [*Enzel et al.*, 2000].

The location of the epicenters of other historical earthquakes can be approximately estimated from the historic reports on the distribution of damage. It should be noted, however, that in older historical periods, time acted as a "high

pass" magnitude filter, and strong and harmful earthquakes were selectively preserved in the written documents [*Ben-Menahem*, 1991]. Thus, a reasonable assumption is that if an earthquake is reported widely in ancient historical records (e.g., 31 B.C. earthquake), it was a high intensity earthquake. The reports on a small magnitude earthquake that did not severely affect the population probably faded away along with other unimportant historical events.

The reports of the 64 B.C. and 33 A.D. earthquakes are very limited. Compared to the 31 B.C. earthquake, these seem moderate and localized. Nevertheless, since most of the reports come from Jerusalem, a reasonable estimation is that the earthquakes occurred on the Jericho Fault (Figures 1 and 4). The 363 A.D. earthquake was probably a stronger earthquake because reports are more extensive, even though they originate only from Israel and western Jordan. However, the deformed unit that was correlated to this event is only a few centimeters thick, implying that the epicenter was probably not as close to the Ze'elim Terrace.

During and after the Crusader period, reports on earthquakes become more frequent [*Ambraseys et al.*, 1994] and they are preserved better than the older historical reports. From the distribution of the historical reports, it seems that the 1212, 1293, 1456, 1546, and 1834 A.D. earthquakes were generated by one of the southern faults of the Dead Sea Graben (Figure 4). Extensive damage from the 1212 A.D. and 1546 A.D. events, reported outside of Israel and Jordan, argues for magnitudes larger than for the 1293, 1456, and 1834 A.D. events. The 1834 A.D. event is a relatively recent event and was reported only in southern Israel, indicating that it produced moderate ground shaking in the Dead Sea area but strong enough to liquefy the sediments in Ze'elim Terrace. The Arava Fault, located on the eastern side of the graben (Figure 1), can be the source for earthquakes located south of the Dead Sea [*Klinger et al.*, 2000].

Although the centers of earthquake damage can be approximately located, it is difficult to assign an earthquake to a particular fault segment. The Jericho and Arava segments of the DST (Figure 1) are expected to be the source of the strongest shocks because they are the largest and most continuous faults in the area [*Garfunkel et al.*, 1981]. However, the entire Dead Sea area is undergoing active deformation [*Garfunkel and Ben-Avraham*, 1996]. As evidence of this, intra-basin faults under the Dead Sea are active and displace the lake floor [*Ben-Avraham et al.*, 1993]. In the Darga fan delta 30 km north of Ze'elim, surface ruptures have been related to late Holocene earthquake events [*Enzel et al.*, 2000]. Post-Lisan deformation is also observed a few km to the west of the study area, on the Ze'elim Terrace, and south of the study area, along the western shores of the southern basin of the Dead Sea [*Agnon*, 1982; *Bartov*, 1999]. It is likely that some of these ruptures act in the postseismic (aftershocks) or preseismic (foreshocks) periods of a large earthquake, hence they do not affect the paleoseismic record. While these and many other questions regarding the seismic activity in the Dead Sea region remain open, our correlation between historical earthquake records and the deformed units in the Ze'elim section provides a new approach in the assessment of paleoearthquakes.

9. Conclusions

The Ze'elim Formation provides an opportunity to reconstruct the paleoseismic record of the last two millennia in the Dead Sea area and to explore the temporal pattern of earthquakes in this part of the Dead Sea Transform. The following conclusions sum up our study:

1.The paleoseismic record of the Dead Sea during the past two millennia was reconstructed based on the identification of deformed layers as seismites.

2. The ground shaking accompanying earthquakes simultaneously affected layers that extended from the lacustrine environment (characterized by laminated aragonite and detritus) to the shore environment (characterized by sand). This induced the formation of mixed layers in the former and liquefied sand in the latter. Lake-level is estimated to have been less than few meters above the sediment surface during times of earthquakes.

3. Eight layers identified as seismites were dated by radiocarbon at Ze'elim Terrace. These seismites are well correlated with the historical record of earthquakes from the area (64 and 31 B.C. and 33, 363, 1212, 1293, 1834, and 1927 A.D.). Other well-documented earthquakes that affected the Dead Sea area do not show up on the Ze'elim sequence. This could be related to distruction of the relvant layers during times of low lake level and erosion. Indeed, all missing earthquakes are correalted with depositional hiatuses in the section.

4. The regional recurrence interval of earthquakes according to the record recovered from the Ze'elim sedimentary section is about 300 years, but when all earthquakes reported in historical records are considered, the recurrence interval is even shorter, about 100 years.

5. The correlation of historical earthquake with dated seismites provides a new approach in the assessment of paleoseismicity. It provides independent geologic documentation of the historical reports and their approximate location and magnitude. By these means, it may be inferred that the epicenters of the 64, 31 B.C. and 33 and 363 A.D. earthquakes were probably located north of the Dead Sea and along the Jericho Fault, while those of the 1212, 1293, 1456, 1548, 1834 A.D. earthquakes were located to the south of the Dead Sea.

Acknowledgments. We wish to thank Nicolas Waldmann, Yuval Bartov, Claudia Migowski, and GSI technicians for their assistance in the fieldwork. The manuscript benefited from the review of Bill Lettis. This research was supported by the German – Israel Foundation for Research and Development (GIF grant #137/95), the Israel-United States Bi National Science Foundation (BSF grant #97-00286), Israel Science Fund (ISF, Grant # 694/95), the Dead Sea Minerva Center and the Ministry of National Infrastructure.

References

Agnon, A., Post Lisan faulting at the Dead Sea graben border, in *Annual Meeting 1982*, p. 1, Israel Geological Society, Elat, 1982.

Allen, J.R.L., *Developments in Sedimentology*, 663 pp., Elsiever Sci. , New York, 1982.

Allen, J.R.L., Earthquake magnitude-frequency, epicentral distance, and soft-sediments deformation in sedimentary basins, *Sediment. Geol.*, *46*, 67-75, 1986.

Ambraseys, N. N. Engineering seismology; earthquake engineering and structural dynamics, *J. Int. Assoc. Earthquake Eng.*, *17*,1-105, 1988.

Ambraseys, N.N., C.P. Melville, and R.D. Adams, *The Seismicity of Egypt, Arabia and the Red Sea: A Historical Review*, 181 pp., Cambridge Univ. Press, New York, 1994.

Amiran, D.H.K., E. Arieh, and T. Turcotte, Earthquake in Israel and adjacent areas: macroseismic observation since 100 B.C.E., *Israel Explor. J.*, *44*, 260-305, 1994.

Arieh, E., An evaluation of six significant historical earthquakes, 24 pp., Seismol. Sec., Geol. Sur. of Israel, Jerusalem, 1977.

Audemard, F.A., and F. Santis, Survey of liquefaction structures induced by recent moderate earthquakes, *Assoc. Eng. Geol. Bull. Int.*, *44*, 5-16, 1991.

Avni, R., The 1927 Jericho earthquake, comprehensive macroseismic analysis based on contemporary sources, Ph.D. thesis, Ben-Gurion Univ. of the Negev, Beer-Sheva, Israel, 1999.

Bartov, Y., The geology of the lisan Formation in Massada and the lisan Peninsula (in Hebrew, abstract in English), The Hebrew University of Jerusalem, Jerusalem, 1999.

Begin, Z.B., A. Ehrlich, and Y. Nathan, Lake-Lisan- The Pleistocene precursor of the Dead Sea, *Geol. Sur. Israel Bull.*, *63*, 30, 1974.

Ben-Avraham, Z., T.M. Niemi, D. Neev, J.K. Hall, and Y. Levy, Distribution of Holocene sediments and neotectonics in the deep north basin of the Dead Sea, *Mar. Geol.*, *113*, 219-231, 1993.

Ben-Menahem, A., Four thousand years of seimicity along the Dead Sea Rift, *J. Geophys. Res.*, *96* 20,195-20,216, 1991.

Ben-Menahem, A., A. Nur, and M. Vered, Tectonics, seismicity and structure of the afro-eurasian junction - the breaking of an incoherent plate, *Phys. Earth Planet. Inter.*, *12*, 1-50, 1976.

Davenport, C.A., and P.S. Ringrose, Deformation of Scottish Quaternary sediments sequence by strong earthquakes motions, in *Deformation of Sediments and Sedimentary Rocks*, edited by M.E. Jones and R.M. Preston, *Geol. Soc. Spec. Publ.*, *29*, 299-314,1987.

Doig, R., Effects of strong seismic shaking in lake sediments, and earthquake recurrence interval, Temiscaming, Quebec, *Can. . Earth Sci.*, *28*, 1349-1352, 1991.

Ely, L.L., R.H. Webb, and Y. Enzel, Accuracy of post-bomb ^{137}Cs and ^{14}C in dating fluvial deposits, *Quat. Res.*, *38*, 196-204, 1992.

Enzel, Y., G. Kadan, and Y. Eyal, Holocene earthquakes in the Dead Sea graben from a fan-delta sequence, *Quat. Res.*, *73/74* 137-144, 2000.

Frumkin, A., M. Magaritz, I. Carmi, and I. Zak, The Holocene climatic record of the salt caves of Mount Sedom, Israel, *Holocene*, *1*, 191-200, 1991.

Garfunkel, Z., Internal structure of the Dead Sea Leaky Transform (rift) in relation to plate kinematics, *Tectonophysics*, *80*, 81-108, 1981.

Garfunkel, Z., and Z. Ben-Avraham, The structure of the Dead Sea basin, *Tectonophysics*, *266*, 155-176, 1996.

Garfunkel, Z., I. Zak, and R. Freund, Active faulting in the Dead Sea rift, *Tectonophysics*, *80*, 1-26, 1981.

Guidoboni, E., A. Comastri, and G. Traina, *Catalogue of Ancient Earthquakes in the Mediterranean Area up to the 10th Century*, 504 pp., Inst. Naz. Geofis., Rome,1994.

Hempton, M.R., and J.F. Dewey, Earthquake-induced deformational structures in young lacustrine sediments, East Anatolian Fault, southeast Turkey, *Tectonophysics*, *98*, T7-T14, 1983.

Kadan, G., Evidence for Dead Sea lake-level fluctuations and recent tectonism from the Holocene fan-delta of Nahal Darga, Israel (in Hebrew, abstract in English), M.Sci. thesis, Ben-Gurion Uni. of the Negev, Beer-Sheva, Israel, 1997.

Kaufman, A., U-series dating of Dead Sea carbonates, *Geochim. Cosmochim. Acta*, *35*, 1269-1281, 1971.

Kaufman, A., Y. Yechieli, and M. Gardosh, Reevaluation of lake-sediment chronology in the Dead Sea basin, Israel, based on new $^{230}Th/U$ dates, *Quat. Res.*, *38*, 292-304, 1992.

Ken-Tor, R., M. Stein, S. Marco, Y. Enzel, and A. Agnon, Late Holocene earthquakes recorded by lake sediments, Ze'elim Plain, Dead Sea, in *Israel Geological Society Annual Meeting, 1998*, edited by R. Weinberger et al., p. 53, Mitzpe Ramon, Israel, 1998.

Klein, C., On the fluctuations of the level of the Dead Sea since the beginning of the 19th century, 83 pp., Hydrol. Serv., Minist. of Agric., Jerusalem, 1961.

Klein, C., Morphological evidence of lake level changes, western shore of the Dead Sea, *Isr. J. Earth Sci.*, *31*, 67-94, 1982.

Klinger, Y., J.P. Avouac, L. Dorbath, N. Abou Karaki, and N. Tisnerat, Seismic behavior of the Dead Sea fault along Araba Valley, *Geophys. J. Int.*, 142, 769-782, 2000.

Marco, S., and A. Agnon, Prehistoric earthquake deformations near Masada, Dead Sea graben, *Geology*, *23* (8), 695-698, 1995.

Marco, S., M. Stein, A. Agnon, and H. Ron, Long-term earthquake clustering: A 50,000-year paleoseismic record in the Dead Sea Graben, *J. Geophys. Res.*, *101*, 6179-6191, 1996.

Migowski, C., R. Ken-Tor, J.F.W. Negendank, M. Stein, and J. Mingram, Post-Lisan record documented in sediment sequences from the western shore area and the central basin of the Dead Sea, paper presented at Terra Nostra 98/6: 3rd ELDP Workshop, sponsor, Ptolemais, Greece, 1999.

Neev, D., and K.O. Emery, *The Destruction of Sodom, Gomorrah, and Jericho: Geological,Climatological, and Archaeological Background*, 175 pp., Oxford Univ. Press, New York, 1995.

Obermeier, S., Using liquefaction induced features for paleoseismic analysis, in *Paleoseismology*, edited by J. McCalpin, Int. Geophys. Ser.,*62*, 331-396, 1996.

Reches, Z., and D.F. Hoexter, Holocene seismic and tectonic activity in the Dead Sea area, *Tectonophysics*, *80*, 235-254, 1981.

Russell, K.W., The earthquake of May 19, A.D. 363, *Bull. Am. Sch. Orient. Res.*, *238*, 47-64, 1980.

Russell, K.W., The earthquake chronology of Palestine and northwest Arabia from the 2nd through the mid-8th century A.D., *Bull. Am. Sch. Orient. Res.*, *260*, 37-59, 1985.

Schramm, A., M. Stein, and S.L. Goldstein, Calibration of the 14C timescale to 50 kyr by 234U-230Th dating of sediments from Lake Lisan (the paleo-Dead Sea), *Earth Planet. Sci. Lett.*, *175*, 27-40, 2000.

Shapira, A., R. Avni, and A. Nur, A new estimate for the epicenter of the Jericho earthquake of 11 July 1927, *Israel J.Earth Sc.*, *42*, 93-96, 1993.

Sims, J.D., Earthquake-induced structures in sediments of Van Norman Lake, San Fernando, California, *Science*, *182*, 161-163, 1973.

Sims, J.D., determining earthquake recurrence intervals from deformational structures in young lacustrine sediments, *Tectonophysics*, *29*, 141-152, 1975.

Stein, M., A. Starinsky, A. katz, S.L. Goldstein, M. Machlus and A. Schramm, Strontium isotopic, chemical and sedimentological evidence for the evolution of Lake Lisan and the Dead Sea, *Geochim. Cosmochim. Acta*, 61, 3975-3992, 1997.

Stuiver, M., P.J. Reimer, E. Bard, J.W. Beck, G.S. Burr, K.A. Hughen, B. Kromer, G. McCormac, J. van-der-Plicht, and M. Spurk, INTCAL98 radiocarbon age calibration, 24,000-0 cal BP, *Radiocarbon*, *40*, 1041-1083, 1998.

Vered, M., and H.L. Striem, A macroseismic study of the July 11, 1927 earthquake, , Isr. At. Energy Comm. Licensing Div. *Rep. IA-LD-1-107*, 18 pp., 1976.

Wells, D.L., and K.J. Coppersmith, New empirical relationship among magnitudes, rupture lenght, rupture width, rupture area, and surface displacement, *Bull. Seismol. Soc. Am.*, *84*, 974-1002, 1994.

Willis, B., Earthquakes in the Holy Land, *Bull. Seismol. Soc. Am.*, *18*, 73-103, 1928.

Yechieli, Y., The effects of water levels change in closed lakes (Dead Sea) on the surrounding groundwater and country rocks, Ph.D. thesis, Weizman Inst., Rehovot, Israel,1993.

Yechieli, Y., M. Magaritz, Y. Levy, U. Weber, U. Kafri, W. Woelfli, and G. Bonani, Late Quaternary geological history of the Dead Sea area, Israel, *Quat. Res.*, *39*, 59-67, 1993.

A. Agnon, Y. Enzel, R. Ken-Tor, and M. Stein, Institute of Earth Sciences, the Hebrew University, Givat Ram, Jerusalem 91904, Israel. (amotz@cc.huji.ac.il; yenzel@vms.huji.ac.il; revital@vms.huji.ac.il; motis@vms.huji.ac.il)

S. Marco, Raymond and Beverly Sackler Faculty of Exact Sciences, Department of Geophysics and Planetary Sciences, Tel Aviv University, Ramat Aviv, Tel Aviv 69978, Israel.

J.F.W. Negendank, GeoForschungsZentrum Potsdam, Telegrafenberg, D-14473 Potsdam, Germany.

(Received January 25, 2000; revised August 11, 2000; accepted August 18, 2000.)